Research Article | Vol. 33, No. 5 / 10 Mar 2025 / Optics Express 10981
Optics EXPRESS

Characterization of free-electron laser third harmonic radiation at FLASH

M. M. Bidhendi,[1,*] I. J. Bermudez Macias,[1,2] R. Ivanov,[1,2] M. V. Yurkov,[1] and S. Düsterer[1]

[1]Deutsches Elektronen-Synchrotron DESY, Notkestr. 85, 22607 Hamburg, Germany
[2]Currently with the European XFEL GmbH, Holzkoppel 4, D-22869 Schenefeld, Germany
[*]mahdi.mohammadi-bidhendi@desy.de

Abstract: The Free-electron LASer in Hamburg - FLASH - generates intense ultrashort pulses with femtosecond duration in the range of 3.3 – 90 nm in the fundamental. In addition, higher harmonic contributions are always present in the spectral distribution, extending this range to much shorter wavelengths. This study presents a detailed exploration of the evolution of the radiation properties of the third harmonic contribution in the self-amplified spontaneous emission (SASE) amplification process. Utilizing a terahertz streaking setup, we measured and analyzed the pulse durations and energies of the fundamental and third harmonic during the amplification process under various operational configurations and compared these with results from the 3D time-dependent free electron laser (FEL) simulation code FAST.

1. Introduction

The interaction of the electron bunch with the extreme ultraviolet (XUV) and x-ray light generated in the undulator of a free electron laser (FEL) leads to the modulation of the electron bunch at the resonant wavelength. This in turn leads to the emission of a powerful, coherent radiation pulse at the fundamental [1–7] as well as small contributions at higher order harmonics ($2\hbar\omega$, $3\hbar\omega, \ldots n\hbar\omega$) mainly due to nonlinearities in the bunching [8–10]. For FELs with planar undulators, harmonics are typically present on the few per mill level [1,11–14].

By now the mechanism of the creation of the harmonic radiation content in FELs and their properties have been extensively studied, both theoretically [8,9,11–13,15] and experimentally [1,10,16–24] in quite some detail. However, a comprehensive experimental comparison of the fundamental and harmonic pulse durations, including their evolution during the amplification process has not been performed to the best of our knowledge. Using the THz streaking setup at FLASH [25] we can measure the pulse duration of the fundamental wavelength as well as the second and third harmonic contribution. In addition, simulations have been performed to get insight into the contributing effects.

Understanding the properties of harmonic radiation is not only of theoretical interest, as many experiments performed at FELs are influenced by higher harmonic radiation. It either generates undesired background or even mimics nonlinear multi-photon interactions [26–28]. On the other hand, many experiments are utilizing the harmonics as they significantly extend the short-wavelength range of the FEL. In particular, investigations in solid samples suffer easily from space-charge effects induced by intense FEL radiation and therefore typically only a fraction of the possible FEL pulse energy is used [29]. In these cases, the flux provided by the harmonics is well sufficient and is frequently used [17,30–33]. Knowing the pulse duration of the harmonic radiation is especially important, as most experiments at FELs are time-resolved studies.

#551587 https://doi.org/10.1364/OE.551587
Journal © 2025 Received 10 Dec 2024; revised 27 Jan 2025; accepted 5 Feb 2025; published 3 Mar 2025

Optics EXPRESS

2. Overview of the radiation properties of the harmonics

For the theoretical study, we consider the case of a free-electron laser with a planar undulator driven by an axisymmetric electron beam. The radiation of the electron beam in the planar undulator contains a rich harmonic spectrum. This refers to both coherent and incoherent radiation. Since odd harmonics of the radiation are resonant on-axis, their intensities are pronounced, while even harmonics are strongly suppressed for the case of axisymmetric electron beams [11,34,35]. The amplification process in a SASE FEL starts from the shot noise in the electron beam, and the radiation at the initial stage is just incoherent undulator radiation. Resonant harmonics are amplified independently in the so-called "linear" (exponential gain) regime [8,36]. This process is referred to as the linear harmonic generation mechanism (LHG).

Figure 1 presents simulations performed using the three-dimensional, time-dependent code FAST [37], illustrating the evolution of radiation power for the fundamental and the third harmonic. The simulation is based on typical FLASH parameters (the same as used in Ref. [38]) including a chirped electron beam as described below. In Fig. 1(a) we see that in the parameter space of FLASH, the fundamental has a much larger gain than the third harmonic. As the amplification of the fundamental approaches the onset of the nonlinear stage (maximum fluctuations in the radiation pulse energy), the density modulation in the electron beam at the higher harmonics becomes more pronounced. This results in a much stronger 3rd harmonic radiation than produced by the LHG mechanism. Starting from the undulator length $z \gtrsim 0.65 z_{sat}$ (where z_{sat} is the saturation length) the nonlinear harmonic generation mechanism (NHG) completely controls the generation of the radiation at higher harmonics. Radiation powers at this point are on the level of $E/E_{sat} \simeq 0.01$ for the fundamental, and $E/E_{sat} \simeq 0.001$ for the third harmonic, respectively (with E_{sat} as the pulse energy emitted at saturation). In practical units, these radiation energies are in the sub-microjoule range for the fundamental, and in the nanojoule range for the third harmonic.

The fluctuations observed in the radiation pulse energy curves reflect the inherent statistical nature of SASE FEL radiation. In the linear stage of amplification, all harmonics are amplified independently, and the statistical properties of the radiation of all frequency harmonics correspond to those of completely chaotic polarized light and are described by Gaussian statistics [39–41]. When an electron beam enters the undulator, its radiation consists of a large number of longitudinal and transverse modes. The mode selection process takes place along the undulator, and radiation energy fluctuations start to grow as $\sigma_E^2 = 1/M$, where M is the number of modes in the radiation pulse. Since the evolution of the fundamental is only slightly disturbed by the harmonics, we can state that its statistical properties are governed by Gaussian statistics up to the undulator length of $z \simeq 0.75 z_{sat}$. In this case, the probability distribution of the instantaneous radiation intensity W follows a negative exponential distribution, and any integral of the radiation intensity (such as radiation power P, or radiation pulse energy E), fluctuates in accordance with the gamma distribution [40,41]:

$$p(W) = \frac{1}{\langle W \rangle} \exp\left(-\frac{W}{\langle W \rangle}\right), \qquad p(E) = \frac{M^M}{\Gamma(M)} \left(\frac{E}{\langle E \rangle}\right)^{M-1} \frac{1}{\langle E \rangle} \exp\left(-M \frac{E}{\langle E \rangle}\right), \tag{1}$$

where $\Gamma(M)$ is the gamma function, with argument $M = 1/\sigma_E^2$, and $\sigma_E^2 = \langle (E - \langle E \rangle)^2 \rangle / \langle E \rangle^2$ is the relative dispersion of the radiation energy. For completely chaotic polarized light, the parameter M has a clear physical interpretation - it is the number of modes in the radiation pulse [40,41].

As depicted in Fig. 1(b), the behavior of the radiation energy fluctuations for the third harmonic differs from that of the fundamental. It is governed by Gaussian statistics up to $z \simeq 0.65 z_{sat}$, after which a rapid increase in fluctuations between $0.65 z_{sat}$ and $0.75 z_{sat}$ is observed. This occurs because the nonlinear harmonics of electron density modulation, driven by the amplification of the fundamental, start to dominate over those generated in the LHG mechanism.

The stage of the amplification process at the onset of the nonlinear regime is a very interesting range, since the third harmonic is produced by the NHG mechanism, while the radiation of

Optics EXPRESS

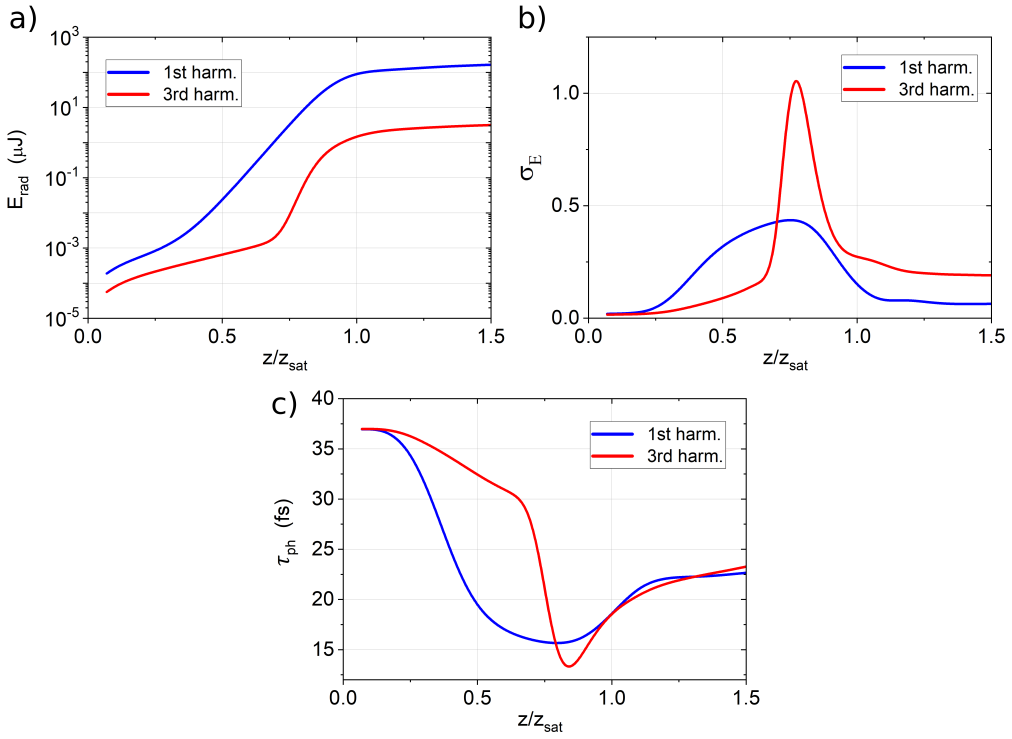

Fig. 1. Simulated gain curves for typical FLASH parameters (details provided in the text). a) Average radiation energy. b) Fluctuations of the radiation pulse energy. c) Evolution of the radiation pulse duration along the undulator. Blue and red colors correspond to the fundamental and the third harmonic, respectively. Results are obtained with the FEL simulation code FAST for an electron bunch with a 5 MeV peak-to-peak energy chirp.

the fundamental is described by Gaussian statistics. It has been noted in Ref. [12] that the statistical properties of harmonic radiation from a SASE FEL change significantly with respect to the fundamental (e.g., with respect to Gaussian statistics). In fact, the radiation intensity of a higher harmonic generated in the NHG process results from the nonlinear transformation of the fundamental intensity, expressed as $z = W^n$. Thus, the negative exponential distribution (Eq. (1)) transforms to [12,42]:

$$p(z) = \frac{z}{n\langle W\rangle} z^{(1-n)/n} \exp(-z^{1/n}/\langle W\rangle) \,. \tag{2}$$

In the nonlinear regime near the saturation point, the probability distributions for both, the fundamental and the 3rd harmonic, change significantly from those in the linear regime. For instance, at saturation, the 3rd harmonic radiation exhibits a much noisier behavior (a nearly negative exponential) for instantaneous intensities, while the fluctuations of the fundamental begin to stabilize [12].

Figure 1(c) shows the evolution of the radiation pulse duration along the undulator for both the fundamental and the third harmonic. In the initial stage of amplification, the radiation is incoherent, thus the radiation pulse profile mimics the electron beam axial profile for all harmonics. As the FEL amplification progresses, the radiation pulse duration begins to shorten since the core of the electron bunch exhibits a higher modulation and produces more radiation power. The minimum pulse duration of the fundamental is achieved at the end of the high gain exponential regime at $z \simeq 0.75 z_{sat}$. After this point, the gain in the central part of the electron

Optics EXPRESS

bunch is saturated while the tail of the bunch (where the amplification process is still in the exponential gain regime) starts to contribute more, leading to the increase of the pulse length by about 40% at the saturation point.

The evolution of the third harmonic pulse duration exhibits a different behavior. When the generation of the third harmonic is driven by the LHG mechanism (for $z \lesssim 0.65 z_{sat}$), the radiation pulse duration is reduced, but at a much slower rate than that of the fundamental. The reason for this is the significantly smaller FEL gain. When the NHG mechanism starts to dominate the harmonic generation, the pulse durations of the fundamental and third harmonic become quite comparable.

Practical estimates of SASE FEL parameters are well described in the framework of the one-dimensional model. We start with the fundamental. The amplification process in SASE FELs starts from shot noise in the electron beam. Radiation power and electron beam modulation grow exponentially until the amplification process reaches the saturation regime. The coherence time grows as well in the exponential gain regime. The saturation point corresponds to the maximum brilliance of the radiation [43]. The saturation length can be described in terms of the FEL parameter ρ and number of cooperating electrons N_c [41,44,45]:

$$z_{sat} \simeq \frac{\lambda_W}{4\pi\rho}\left(3 + \frac{\ln N_c}{\sqrt{3}}\right) \quad , \tag{3}$$

where $N_c = I/(e\rho\omega)$, ω is the radiation frequency, I is the beam current, $-e$ is the charge of electron, and λ_W is undulator period. The coherence time at saturation is given by

$$(\tau_c)_{max} \simeq \frac{1}{\rho\omega}\sqrt{\frac{\pi \ln N_c}{18}} \, . \tag{4}$$

A practical estimate for the parameter ρ can be made based on the observation that in the parameter range of SASE FELs operating in the XUV and x-ray wavelength range, the number of field gain lengths to reach saturation is about 10 [43]. Thus, the parameter ρ and the coherence time τ_c relate to the saturation length as:

$$\rho \simeq \lambda_W / z_{sat}, \quad \tau_c \simeq \lambda z_{sat}/(2\sqrt{\pi} c \lambda_W). \tag{5}$$

We consider an electron beam with a longitudinal Gaussian profile with an rms duration τ_{el}. The radiation pulse duration is mainly determined by the length of the lasing fraction of the electron bunch with additional corrections related to the slippage effect. The minimum pulse duration (τ_{ph}^{min} in FWHM) is reached at the end of the high-gain linear regime [46]:

$$\tau_{ph}^{min} \simeq 0.4\tau_{el} \simeq 0.7 \times M \times \tau_c \, . \tag{6}$$

The figure of merit for describing the radiation properties of the higher harmonics is the coupling factor K_h:

$$K_h = K(-1)^{(h-1)/2}[J_{(h-1)/2}(Q) - J_{(h+1)/2}(Q)] \, , \tag{7}$$

where $Q = K^2/[2(1+K^2)]$, K is the undulator parameter, and J is the Bessel function. In the saturation point, the radiation powers for the 3rd and 5th harmonics are related to the power of the fundamental as [12]:

$$\frac{\langle W_3 \rangle}{\langle W_1 \rangle}|_{\rm sat} = 0.094 \times \frac{K_3^2}{K_1^2} \, , \qquad \frac{\langle W_5 \rangle}{\langle W_1 \rangle}|_{\rm sat} = 0.03 \times \frac{K_5^2}{K_1^2} \, . \tag{8}$$

with relevant corrections for emittance and energy spread effects.

Optics EXPRESS

At the saturation point, the coherence time for higher harmonics decreases approximately in inverse proportion to the harmonic number n, while the relative spectral bandwidth remains nearly the same for all harmonics.

This model describes the SASE process in FLASH rather well. Experimental results of extended studies of harmonic generation at FLASH have been presented e.g. in Ref. [1]. In these studies, the fundamental wavelength was 13.7 nm. The contribution of the odd harmonics was in agreement with theoretical expectations, of approximately 0.6% and 0.03% for the 3rd (4.6 nm) and the 5th (2.75 nm) harmonics, respectively.

Looking at even harmonics, it is to note that the harmonic bunching factor is highest for the second harmonic, but due to the symmetry of the planar undulators, the on-axis radiation at even harmonics is strongly suppressed, since the contributions from neighboring periods are out of phase and cancel each other out due to destructive interference. Consequently, the radiation of even harmonics is significantly suppressed in a SASE FEL with a planar undulator driven by an axisymmetric electron beam [11,34,35]. The measurements of even harmonics presented in Ref. [1] have shown that they were indeed much weaker compared to the odd harmonics, since these measurements have been performed with careful tuning of the machine parameters such as the beam formation system, orbit, optics, dispersion, etc. However, sometimes measurements show non-negligible levels of the 2nd harmonic [20] as well as in the present work. This happens when not all machine parameters are tuned in a controlled way leading to an asymmetry in the radiating system. Due to a finite electron beam size, betatron motion inside the undulators as well as a not perfectly straight trajectory (and possibly other reasons) the destructive interference is limited, leading to significant second harmonic radiation. Unfortunately, the properties of the 2nd harmonic cannot be described quantitatively due to insufficient knowledge of imperfections, allowing only a qualitative discussion of potential effects [11,35,36,47].

The statistical properties of the 2nd harmonic are governed by the NHG mechanism similar to those of odd harmonics. Regarding the radiation pulse duration, within the NHG-controlled range it should evolve similarly to the fundamental. A quantitative description is only possible with precise knowledge of the asymmetries. Detailed experimental studies of the 2nd harmonic radiation are a delicate subject and require dedicated setups that also account for the specific angular distribution of the radiation.

3. Simulation of the SASE process

The analysis of the FLASH2 operation indicates that the value of the normalized rms emittance of the electron beam is in the range between 1 and 1.4 mm-mrad. Typically, at 13.5 nm, the machine reaches saturation after seven undulator modules when operating with a 1 GeV electron beam energy. This corresponds to the value of the peak electron beam current in the range from 1 to 1.5 kA. Based on multiple spectral measurements conducted at FLASH, the measured FEL bandwidth is typically around 1% FWHM [1,48–50], which is notably wider than the natural FEL bandwidth of approximately 0.4–0.5% for the given parameter space. This doubling of the natural bandwidth arises from the energy chirp along the electron bunch. Using the frequency chirp characterization method based on THz streaking, outlined in Ref. [51], we measured a chirp for the data shown in this publication that resulted in a broadening factor ranging from 1.8 to 2.3 times the natural bandwidth, which is in good agreement with the spectral measurements. Building on these findings, the the chirp in the simulation was adjusted such that the natural line width is doubled leading to a spectral width of approximately 1%.

There are several mechanisms of chirp generation. Long pulse, low current electron beam produced in the electron gun is compressed in several stages by a large factor (up to about one hundred), and the peak current is increased correspondingly [52]. To achieve such a compression, an energy chirp along the electron bunch is applied in the accelerating sections. This energy chirp leads to bunch compression when the electron bunch moves through dedicated magnetic

Optics EXPRESS

bunch compressors. The RF-induced energy chirp can be minimized such that it only slightly changes the FEL properties with respect to a monoenergetic beam. On the other hand, different kinds of wakefields and collective effects also generate an energy chirp along the electron bunch. In particular, the longitudinal space-charge field (LSC) [52] has a strong effect on the energy chirp. An important feature of the LSC wake is that the energy of the electrons in the lasing fraction of the electron bunch is increased from the tail to the head of the electron bunch. This feature results in a visible increase in FEL efficiency in the nonlinear regime, at the cost of an increase in the FEL radiation bandwidth. The radiation pulse duration is also affected by this kind of energy chirp. During the experiments discussed in this paper, the beam formation system was typically tuned such that the LSC produced a significant energy chirp, resulting in the increase of the radiation spectrum bandwidth by about a factor of 2 compared to the natural FEL bandwidth.

Thus, the simulations have been performed with the three-dimensional, time-dependent simulation code FAST [37] for an electron energy of 1 GeV including a 5 MeV peak-to-peak energy chirp, an rms energy spread of 0.2 MeV and a rms normalized emittance of 1.4 mm mrad. The lasing fraction of the electron bunch is approximated with a Gaussian distribution of about 16 fs rms pulse duration and a 1.5 kA peak current, resulting in a radiation wavelength of 13.5 nm. The same simulation parameters have already been used in Ref. [38], where a good agreement between simulation and experiment has been shown over a rather large experimental parameter range.

4. Experiment

4.1. Setup description

To obtain information on the XUV pulse duration and pulse energy for both the fundamental and its third harmonic (and to some extent the second harmonic), we used THz streaking [53,54]. The THz streaking technique employs a noble gas target, which is photoionized by the FEL pulses. The resulting photoelectrons carry the temporal and spectral characteristics of the ionizing XUV radiation. These photoelectrons propagate within the time-varying electric field of a co-propagating THz radiation and the final photoelectron kinetic energy distribution is measured by an electron time-of-flight (eTOF) spectrometer. Depending on the time of ionization with respect to the THz field, the photoelectrons change their momentum component in the polarization plane of the THz field. If the electron wave packet is short compared to the period length of the THz field, the temporal structure of the electron wave packet will be mapped onto the kinetic energy distribution of the emitted electrons and thus can be used to determine the pulse duration (details are described e.g. in Ref. [55,56]). Since the number of detected photoelectrons was proportional to the XUV photons interacting with the gas target, we could use the photoelectron spectra as the pulse energy monitor as well, similar to the approach outlined in Refs. [57,58].

The measurements were performed at the dedicated photon diagnostic beamline FL21, which is equipped with a permanently installed THz streaking setup [25]. The setup consists of an interaction chamber in which the XUV and the THz beams are focused co-linearly to the interaction point that is monitored by two eTOFs opposing each other perpendicular to the propagation direction of the XUV pulses. A dedicated laser system delivers about 1 ps long pulses at 1030 nm with a pulse energy of 3.5 mJ at a repetition rate of 10 Hz. These laser pulses are used to generate the THz radiation based on optical rectification using a nonlinear crystal ($LiNbO_3$) (for details see e.g. [56,59]).

To accurately determine the streaking effect for each XUV pulse while avoiding space-charge-induced spectral broadening, the single-shot streaked photoelectron signal must be sufficiently intense, but not excessive to avoid a too large amount of ions created in the FEL focal volume. Because of the large collection efficiency of the eTOF (Kaessdorf ETF11) and the high cross section of noble gases in the XUV regime, only few 100 nJ of pulse energy are needed to

Optics EXPRESS

accurately measure the kinetic energy distribution of the photoelectrons [56]. The low pulse energy requirement allows the measurement of even the weak harmonic content of the FEL radiation. Since the harmonics typically only contain a fraction of a percent of the fundamental radiation, the latter one has to be suppressed substantially to be able to monitor the harmonic signal without tremendous space-charge effects of the fundamental. Therefore, thin metal filters (such as 200 nm zirconium in the present case) must be used to reduce the intensity of the fundamental wavelength significantly (see Fig. 2). This ensures an accurate measurement of the higher harmonics alongside the fundamental. Due to the strongly attenuated fundamental and a rather large XUV focal spot of ~ 100 µm, we can exclude the possibility of multiphoton processes contributing to the observed signals.

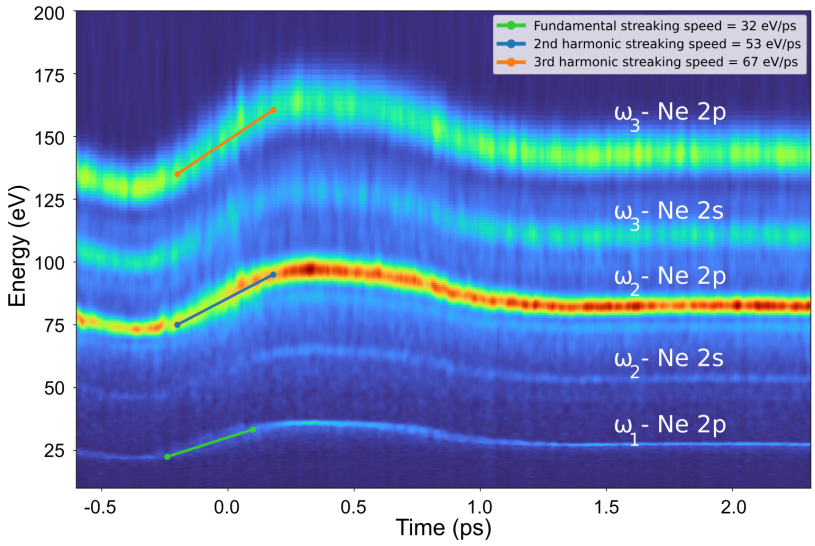

Fig. 2. Kinetic energy of neon 2p and 2s photoelectrons induced by the fundamental, second and third harmonic radiation of FLASH. The photoelectrons are created in the presence of the THz streaking field, plotted as a function of the time delay between the FEL and THz pulses. The fundamental FEL wavelength was set to 24 nm (52 eV), leading to a second harmonic of 12 nm (104 eV) and a third harmonic of 8 nm (155 eV). The fundamental radiation is strongly suppressed by a 200 nm thick Zr filter. The 'streaking speed' is derived from the slope of the linear segment in each streaking trace.

4.2. Pulse duration measurements

In Fig. 2, the kinetic energy spectra of photoelectrons created by the fundamental, second and third harmonic are plotted as a function of the temporal delay between the XUV and THz pulses. This delay scan, often called the 'streaking trace,' is directly proportional to the vector potential of the THz field. The streaking trace provides the maximum energy shift of photoelectrons for a given THz field and electron kinetic energy. By fitting the linear segment of the streaking trace (shown as solid lines in Fig. 2), we can determine the 'streaking speed', a parameter that connects the energy shift with the emission time [56,60]. Note, that the streaking speed increases (for the same THz field) with the kinetic energy of the electrons as $\sqrt{E_{kin}}$ [55]. The pulse durations were analyzed following the method described in Ref. [51], with the chirp taken into account.

FLASH can be operated in a large range of parameters regarding wavelength, pulse energy, pulse duration, etc. Thus, the pulse durations of the fundamental and the third harmonic were not only measured for a specific setting but utilizing the benefit of a permanently installed diagnostics

Optics EXPRESS

endstation [25] several different FEL configurations were used. As illustrated in Fig. 3 the fundamental (blue points) and the third harmonic (red points) pulse durations were measured as a function of the amplification along the undulator.

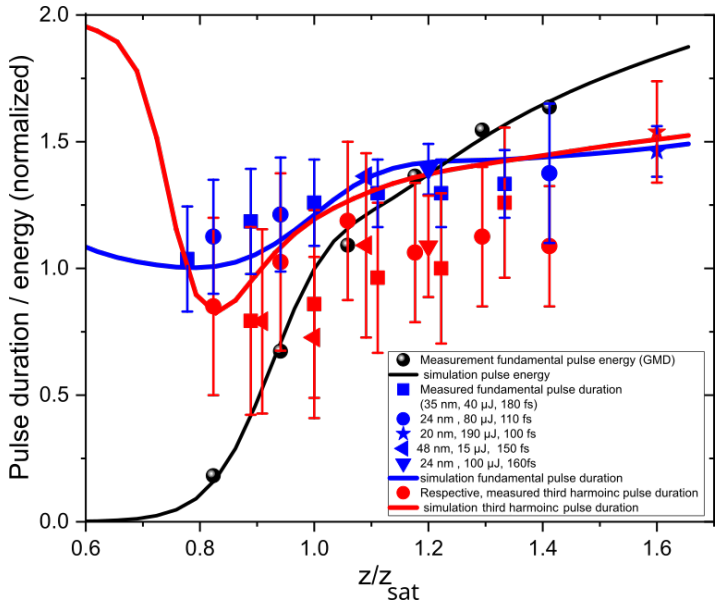

Fig. 3. Evolution of the measured pulse duration for the fundamental and the third harmonic for various FEL settings compared to the simulation. The experimental data was acquired over a period of several years for different FEL settings (see legend). For each data point ~ 3000 pulses of τ_{ph}^{1st} and τ_{ph}^{3rd} have been measured with THz streaking. To compare the individual measurements the fundamental pulse durations of each setting have been scaled to the simulation and the same scaling factor was applied to the third harmonic durations. The 'error bars' do not show the experimental uncertainty, but rather the rms width of the observed pulse duration distribution caused by SASE-based fluctuations, 'technical' fluctuations as well as measurement errors to demonstrate how much the FEL pulse duration changes for a particular setting. The simulated values (lines) are the 3D FAST simulations for a chirped electron pulse, as shown in Fig. 1.

Analog to the scheme outlined in Ref. [38] the undulators were opened one by one and the experimental conditions (XUV pulse energy and suppression of the fundamental) were optimized for each setting. In total, we measured the complete gain curve or at least parts of it in several different measurement campaigns distributed over few years. Thus, we cover a large range of FEL settings with fundamental wavelengths from 20 to 48 nm, for pulse durations in the range of 100 fs to 180 fs and saturation energies of 15 μJ to almost 200 μJ.

The experimentally determined pulse durations of the third harmonic (red points) and the fundamental (blue points) for a large parameter range are presented in Fig. 3 together with the simulation result as solid lines. To compare the different settings, the pulse durations of the fundamental and the pulse energies were scaled to the FAST simulation. The scaling process followed the method described in Ref. [38], as the simulation result for the fundamental provides a reasonably accurate description of the evolution of the pulse duration along the undulators, despite differences between the experimental and simulated parameters.

The number of undulators was scaled to the undulator coordinate z, ensuring that the onset of measurable SASE (>0.5 μJ) aligns with the z range in which the energy gain becomes visible in the simulated energy gain curve ($z/z_{sat} \sim 0.7$). This establishes the scaling for the undulator axis

Optics EXPRESS

and defines the saturation length z_{sat}. Subsequently, the pulse energy was scaled such that at $z = z_{sat}$, the pulse energy was defined as the saturation pulse energy E_{sat}, and all energies were normalized to this value. Since we typically have fewer measurements for the pulse duration than we have for the pulse energy, we cannot normalize the pulse durations as systematically as the pulse energy. Thus, we chose the approach to scale the pulse durations of the fundamental for each experimental setting to minimize the deviation to the simulation and use this factor to subsequently scale the third harmonic duration.

Due to the lack of theoretical predictions for comparison, the second harmonic pulse duration was not systematically studied. However, for a few cases second harmonic data was taken, showing that the second harmonic pulse duration had about the same pulse duration as the third harmonic, thus slightly shorter than the fundamental.

4.3. Pulse energy in the harmonic

Typical XUV pulse energies for the fundamental are in the range of tens to hundreds of μJ for FLASH while the second and third harmonic radiation is expected to be on the order of 0.2-2%, thus in the nJ or low μJ range [12]. See also Ref. [21] for a comprehensive analysis of the second and third harmonic at the European XFEL.

The determination of the actual pulse energy ratios of the harmonics and the fundamental radiation at the exit of the undulator is indeed not as easy as it may look at first glance at Fig. 2. Here one can rather easily determine the different signal amplitudes for the fundamental, second and third harmonic. However one has to consider several factors that influence this ratio on the way between the undulator exit to the detector of the eTOF.

First of all the fundamental radiation is attenuated by the so-called gas attenuator, in order to reduce the amount of FEL photons that reach the THz streaking setup. The attenuator consists of a $\sim$ 15 m long part of the XUV beamline which can be filled with up to few times 10^{-2} mbar of gas (noble gas or, as in the present case, nitrogen) that typically has significantly different cross-sections for the fundamental and the harmonics (here we consider the wavelength range of 25 nm- 35 nm). Following the Lambert-Beer law we can determine the attenuation which can be many times higher for the fundamental than for the harmonics for high gas pressures in the attenuator. The second influence to consider is the presence of 5 mirrors in the beam path (3x carbon coated + 2x gold coated) with only a small wavelength dependence in the measured range but significant influence for shorter wavelengths.

An additional source of influence is the wavelength-dependent cross-section of the target gas (Ne), which is about 2-4 times larger for the fundamental than for the harmonics [62]. In addition, the asymmetry parameter β, indicating the angular distribution of the photoelectrons, changes over the considered wavelengths range by a factor of about 2 [62]. Electrons ejected by shorter wavelength radiation are more predominately emitted along the polarization axis of the XUV and thus are more efficiently collected by the eTOF.

Finally, to get a sufficient eTOF signal for the harmonic radiation, the electrostatic lens in the eTOF has to be optimized for a good transmission for faster electrons, which leads again to a change of the fundamental to harmonic signal ratio in the range of 10. This enhancement factor can be determined by measuring the ratio with and without a lens for a strong harmonic signal (in deep saturation). Furthermore one has to consider that the measured signal by the eTOF is proportional to the number of photons present in the harmonic or the fundamental. Thus, to get the ratio in pulse energy (μJ) one has to multiply the determined ratios by 2 for the second and 3 for the third harmonic. Using all corrections leads to rather a large uncertainty which we estimate to be about $\pm$ 50%.

We do not consider the possible difference in pointing and divergence of the fundamental and the harmonics, since typically most of the radiation propagating along the beamline is collected by the focusing mirror and is focused on the interaction point.

Optics EXPRESS

4.3.1. Pulse energy measurement

The second and third harmonic ratios vary a lot each time the FEL is set up for a new operation point (different pulse duration, wavelengths, pulse energy, etc.). Looking at the large number of measurements taken over a period of several years, we find the second harmonic ratio range at ~ 0.1-0.6% and the third harmonic ratio at ~ 0.2-0.6% compared to the fundamental pulse energy. Measurements with a grating spectrometer have determined values up to 1% for FEL settings specifically optimized for the third harmonic. The determined third harmonic range is also in agreement with Eq. (8), predicting a maximum third harmonic contribution between 0.9% (for $K \sim 1$) and 1.8% (for $K \sim 2$) within the K (undulator parameter) range used in the experiments (see Ref. [8]). Here one has to take into account that the typical energy spread suppresses the third harmonic up to a factor of 3 in the practical case [12] decreasing the maximum values to the range of the experimentally determined ratios. In the future, a third harmonic afterburner undulator will further enhance the radiation output at the third harmonic at FLASH2 [63].

The development of the FEL pulse energy along the undulators is illustrated in Fig. 4(a). The simulation (solid lines) suggests that, at the end of the linear amplification regime of the fundamental, NHG mechanism governs the generation of the third harmonic such that the power of the third harmonic increases more rapidly than the power of the fundamental. Therefore, according to the simulation, to achieve a high-intensity third harmonic, the FEL likely needs to be tuned for saturation or even better deep saturation regime. Experimental data suggest a similar trend to that indicated by the simulation. However, the absolute values of the harmonic energies are lower than predicted by the simulation. A possible reason is that the measurement was taken for a standard FEL setup that was not tailored for harmonic emission. The second harmonic radiation is in addition to the third harmonic signal also recorded in the eTOF traces. Thus, we can present the measured values, which are typically rather similar to the third harmonic, but due to limited knowledge about non-symmetry in the radiating system that leads to the generation of the second harmonic, no simulation was performed.

4.3.2. Pulse energy fluctuations

Since the pulse energy is measured for each FEL pulse, we extended the analysis from the average pulse energies shown in Fig. 4(a), to the pulse-to-pulse energy fluctuations as shown in Fig. 4(b). The fluctuation (rms of the pulse energy normalized to the average pulse energy) of the fundamental and third harmonic pulse energy are plotted along the undulators and compared with the simulation. The simulation predicts that the fluctuation increases in the linear regime to a maximum at about $z/z_{sat} \sim 0.8$, where the fundamental and third harmonic reach their maximum fluctuation and subsequently the fluctuations are strongly suppressed in saturation [12,40]. While the third harmonic shows lower fluctuations than the fundamental in the very early part of the amplification it has a much stronger increase and exceeds the fluctuations of the fundamental by factor ~ 2.5 at $z/z_{sat} \sim 0.8$. The fluctuations of the third harmonic, however, stay about 2.5 higher than the fundamental fluctuations in deep saturation, since in this regime the third harmonic is governed by the NHG while the fundamental radiation follows Gaussian statistical behavior. Thus, to obtain a third harmonic pulse with reduced fluctuations, the FEL should operate in the saturation and deep saturation regime. The measured fluctuations exceed the theoretically predicted values, mainly due to measurement uncertainties and additional technical fluctuations during the acceleration process, as discussed in detail in Ref. [61].

4.4. Single-pulse correlations

4.4.1. Pulse energy correlation

Recording the pulse energies for each FEL pulse at the fundamental and the third harmonic enables the investigation of any correlation between them. The pulse energy of the fundamental radiation

Optics EXPRESS

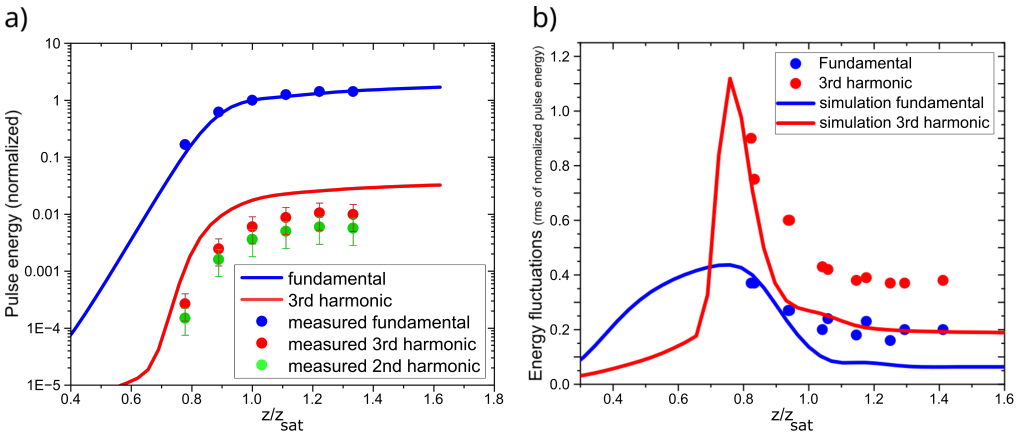

Fig. 4. a) Evolution of the pulse energy for the fundamental, second and third harmonic, displayed on a logarithmic scale, as a function of the undulator length on a linear scale (symbols are experimental data, lines are from the FAST simulation). All data points were normalized on the fundamental pulse energy at the onset of saturation ($z/z_{sat} = 1$). The estimated error for the harmonic experimental data is ±50% - see text. b) Fluctuations of the pulse energy for the fundamental and the third harmonic as a function of undulator length, comparing experimental data with simulation results. The experimental data shows larger fluctuations than the theoretically expected values, which can be attributed to measurement uncertainty and additional technical fluctuations in the accelerator, as discussed in Ref. [61]. The third harmonic shows about a factor of 2.5 larger energy fluctuation than the fundamental at $z/z_{sat} = 0.8$ and beyond. This difference arises in the saturation regime, as the third harmonic is produced by the NHG mechanism, while the fundamental is described by Gaussian statistics.

was measured using a gas monitor detector (GMD) [57,64] upstream of the THz streaking (which has a measurement precision of ∼ ±5%). The energy of the third harmonic is derived from the signal intensity measured by the eTOFs. The single-shot energies of the fundamental and third harmonic along the undulators are shown in Fig. 5(a) to (d). The experimental data shows no correlation between the pulse energy of the third harmonic and fundamental. Still, one can see the decrease of the fluctuations as the amplification process advances (as shown in Fig. 4(b)). The simulation predicts a linear correlation between the pulse energies of the fundamental and third harmonic in the linear regime. However, this linear correlation was not observed experimentally, probably due to the larger measurement uncertainties in this regime.

4.4.2. Pulse duration correlation

Additionally, the pulse duration of the third harmonic was measured pulse resolved with THz streaking and, thus, can be compared with the pulse energy of the third harmonic. The result together with the simulation is shown in Fig. 5(e) to (h) at different stages of the amplification process. The simulation suggests that fluctuations in pulse energy are approximately twice as large as those in pulse duration. The experimental data confirm this but with broader fluctuations as seen in Fig. 4(b). The simulation as well as the experimental results indicate no clear correlation between the pulse duration and pulse energy of the third harmonic in or close to saturation. On the other hand, the simulation predicts an interesting relation for the early amplification stage ($z/z_{sat} = 0.76$) for which we unfortunately do not have sufficient experimental data due to the low signal level at $z/z_{sat} = 0.76$.

Optics EXPRESS

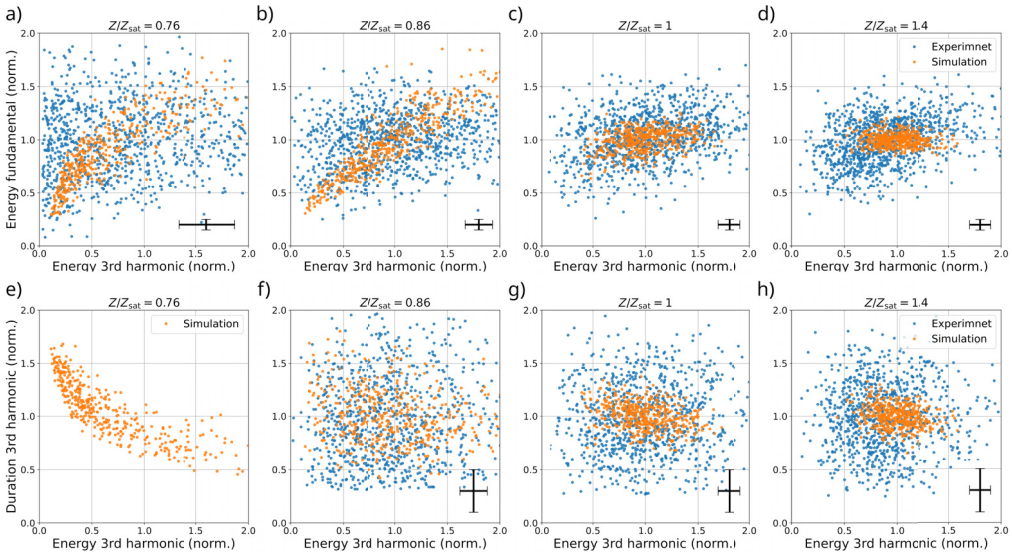

Fig. 5. The upper row shows the experimental and simulated data the for single-shot pulse energy of the fundamental and third harmonic, at different stages of amplification. All shown data is normalized to the respective mean value. The experimental data does not show a correlation. The lower row shows experimental and simulated data for the pulse duration and pulse energy of the third harmonic. In e), the experimental result is not shown since the third harmonic signal was too low for a reliable pulse duration measurement.

5. Discussion

In Ref. [38] we compared the evolution of the fundamental pulse duration and energy along the undulator with predictions from a 3D FEL simulation (FAST code), using standard FLASH settings including a chirped electron beam. There was a remarkable agreement of the measurements with the simulation despite the simulation being performed for one specific case and the measurements spanned over a rather large parameter range (wavelengths from 8 nm to 34 nm). As shown in Ref. [38] the addition of a chirp in the electron bunch simulation leads to much better agreement with the experimental data. Here we extended the approach by including the pulse duration and energy of the third harmonic content of the FEL radiation. And again we find a reasonable agreement between the simulation results and the measurements.

Figure 3 shows the photon pulse duration for the fundamental and the third harmonic radiation as a function of the undulator coordinate z. The simulation shows that the pulse duration of the fundamental is rather constant in the linear regime (z/z_{sat}<0.8) and increases towards the end of the linear regime by only $\sim$ 30% and stays almost constant in saturation (in contrast to the unchirped simulation where the pulse duration strongly increases in saturation [38]). The third harmonic pulse duration has a more interesting behavior. In the linear regime it is actually longer than the fundamental. In this regime, the generation of the third harmonic is primarily driven by the LHG mechanism (up to $z \approx 0.65 z_{sat}$). Therefore, the third harmonic pulse duration remains longer than that of the fundamental. This slower reduction in duration is attributed to the smaller FEL gain for the third harmonic compared to the fundamental. However, as the NHG mechanism begins to dominate (around $z \gtrsim 0.65 z_{sat}$), the third harmonic experiences enhanced amplification driven by nonlinear density modulation effects. After the saturation point, the simulation predicts that the pulse duration of the fundamental and the third harmonic are about identical. This is indeed surprising if one compares this with seeded FELs where the nth harmonic of the seed laser leads to an FEL pulse duration scaling (in the simplest approach) as $1/\sqrt{n}$ [65] and the same

Optics EXPRESS

scaling applies for the harmonic generation of optical pulses in a nonlinear crystal (again in a simple approach) [66].

The experimental data shows a large variation of the third harmonic pulse durations which can be attributed to the widely different experimental settings for each experimental campaign. Still, it shows a similar trend as the simulation, namely a slight pulse duration elongation from linear range to deep saturation. However, looking at the actual third harmonic pulse durations, they are on average $\sim 20\%$ shorter as compared to the fundamental, and thus slightly shorter than anticipated by the simulation. This may be due to a not fully optimized electron bunch phase space for the standard operation.

Looking at the pulse energy, the simulation result shown in Fig. 4(a) predicts that in the linear regime, the third harmonic's energy rises significantly faster compared to the fundamental. Upon reaching the saturation regime, the increase in pulse energy for both the fundamental and the third harmonic slows down. The experimental data follows a similar trend but with lower overall energy values, which again can be caused by unoptimized FEL settings.

Utilizing the third harmonic in FEL experiments it is not only important to know the pulse energy but also its fluctuations. The energy fluctuations shown in Fig. 4(b) indicate that the fundamental and third harmonic reach their maximum fluctuation at the end of the linear regime at $z/z_{sat} = 0.8$ [12]. Both theory and experiment show that the fluctuation decreases strongly afterwards. It is to be noted that the energy fluctuations of the third harmonic are at the end of the linear regime till deep saturation about 2.5 times larger than the ones for the fundamental, thus making measurements using the third harmonic more challenging.

Summarizing the findings so far, the best operation point (not considering transverse beam properties) for decent third harmonic radiation at FLASH is in deep saturation. The pulse energy is still growing in saturation for a (negatively) chirped electron bunch while the fluctuations are constantly low and the pulse duration only increases slightly.

Since the THz streaking measures the pulse energy and pulse duration for each photon pulse, we can also look for correlations between different radiation properties. In Ref. [61] we looked at correlations between various properties of the fundamental radiation and found no significant correlations in saturation either in the simulation or in the experimental data. Looking at Fig. 5 we also find no defined correlation for the pulse energy or pulse duration of the third harmonic in saturation. However, the simulation predicts a strong correlation between the fundamental and the third harmonic pulse energy in the linear regime, which is not represented in the experimental data. Even having the large error bars, we should be able to see a certain degree of correlation in the data and it is up to now not understood why it was not observed. Looking at the exponential gain regime there is a negative correlation between the third harmonic pulse energy and pulse duration (analog to the simulations for the fundamental presented in Ref. [61]) as shown in Fig. 5(e). The pulse duration tends to be shorter for pulses with larger energy. Unfortunately, due to the low signal-to-noise ratio at $z/z_{sat} = 0.76$, we were not able to measure the pulse duration and compare with the prediction.

Generally, the absence of correlation for the saturated pulses is advantageous for data analysis. When sorting the experimental dataset according to one radiation property there is no undesired spurious correlation with another property which could lead to false correlations in the sorted experimental data.

Considering that the simulation was performed for quite different FEL parameters the agreement is rather remarkable. In several cases, the measured performance was less than in the (perfect) simulations which we attribute to not fully optimized FEL settings. This may sound like a drawback for the comparison with the theoretical predictions, but we deliberately measured with the standard settings that are present for all-day operation, to document the parameters available for experiments without dedicated optimization of certain parameters. This way we get a good

Optics EXPRESS

estimation of the variation of parameters and how well the theoretical predictions can be used for the planning of future experiments.

6. Conclusion

We analyzed the evolution of the pulse duration and pulse energy of the fundamental and third harmonic radiation of FLASH during the amplification process. Using THz streaking as a detection method, measurements were taken for a large range of FEL parameters from 20 nm to 48 nm, for pulse durations in the range of 100 fs to 180 fs and saturation energies of 15 μJ to almost 200 μJ for the fundamental radiation. The experimental results were compared to 3D simulations (FAST code) simulating a chirped electron bunch, similar as described in Ref. [38]. Due to the large parameter range, the measurements show some variation, but in general we can state that the third harmonic pulse duration is about 20% shorter as compared to the fundamental, with a pulse energy ratio to the fundamental ranging from 0.2% to 0.6%. The pulse durations of fundamental and third harmonic increase from the onset of saturation to deep saturation only slightly due to the electron chirp which is typically present at FLASH. The energy fluctuations of the third harmonic decrease from the end of the linear regime to deep saturation but stay for the whole range about 2.5 times higher than the fluctuations of the fundamental. Looking at correlations between pulse energy and pulse duration we found experimentally no significant correlations between the properties (similar to investigations in Ref. [61]). In contrast, the simulations predict correlations in the early stage of the amplification which are experimentally not easily accessible. Despite the differing FEL parameters used in the simulation and the experiments, the agreement between the measured data and the simulations is decent. Thus, the predictions of the simulation can be used for a large parameter range to guide future FEL experiments.

Funding. Deutsche Forschungsgemeinschaft (491245950).

Acknowledgments. We acknowledge DESY (Hamburg, Germany), a member of the Helmholtz Association HGF, for the provision of experimental facilities. This research was carried out at FLASH. Particularly, we want to acknowledge the work of the scientific and technical team at FLASH for helpful discussions and for fulfilling our special wishes during our beamtimes. We also like to acknowledge Ulrike Frühling for useful discussions and suggestions for improving this article. We also thank Marion Kuhlmann for providing information on spectral measurements of higher harmonics. This work was partially funded by the Helmholtz Association IVF fund under project InterLabs-0002 "HELPFEL."

Disclosures. The authors declare no conflicts of interest.

Data availability. The data presented in this study are available on request from the corresponding authors.

References

1. W. Ackermann, G. Asova, V. Ayvazyan, *et al.*, "Operation of a free-electron laser from the extreme ultraviolet to the water window," Nat. Photonics **1**(6), 336–342 (2007).
2. P. Emma, R. Akre, J. Arthur, *et al.*, "First lasing and operation of an ångstrom-wavelength free-electron laser," Nat. Photonics **4**(9), 641–647 (2010).
3. D. Pile, "First light from SACLA," Nat. Photonics **5**(8), 456–457 (2011).
4. T. Ishikawa, H. Aoyagi, T. Asaka, *et al.*, "A compact X-ray free-electron laser emitting in the sub-ångström region," Nat. Photonics **6**(8), 540–544 (2012).
5. E. Allaria, R. Appio, L. Badano, *et al.*, "Highly coherent and stable pulses from the FERMI seeded free-electron laser in the extreme ultraviolet," Nat. Photonics **6**(10), 699–704 (2012).
6. M. Altarelli, "The European X-ray free-electron laser facility in Hamburg," Nucl. Instrum. Methods Phys. Res., Sect. B **269**(24), 2845–2849 (2011).
7. B. D. Patterson, R. Abela, H.-H. Braun, *et al.*, "Coherent science at the SwissFEL x-ray laser," New J. Phys. **12**(3), 035012 (2010).
8. Z. Huang and K.-J. Kim, "Three-dimensional analysis of harmonic generation in high-gain free-electron lasers," Phys. Rev. E **62**(5), 7295–7308 (2000).
9. H. P. Freund, S. G. Biedron, and S. V. Milton, "Nonlinear harmonic generation and proposed experimental verification in SASE FELs," Nucl. Instrum. Methods Phys. Res., Sect. A **445**(1-3), 53–58 (2000).
10. S. G. Biedron, R. J. Dejus, Z. Huang, *et al.*, "Measurements of nonlinear harmonic generation at the Advanced Photon Source's SASE FEL," Nucl. Instrum. Methods Phys. Res., Sect. A **483**(1-2), 94–100 (2002).
11. G. Geloni, E. Saldin, E. Schneidmiller, *et al.*, "Exact solution for second harmonic generation in XFELs," Opt. Commun. **271**(1), 207–218 (2007).

Optics EXPRESS

12. E. L. Saldin, E. A. Schneidmiller, and M. V. Yurkov, "Properties of the third harmonic of the radiation from self-amplified spontaneous emission free electron laser," Phys. Rev. Spec. Top.–Accel. Beams **9**(3), 030702 (2006).
13. E. A. Schneidmiller and M. V. Yurkov, "Harmonic lasing in x-ray free electron lasers," Phys. Rev. Spec. Top.–Accel. Beams **15**(8), 080702 (2012).
14. E. A. Schneidmiller and M. V. Yurkov, "Coherence Properties of the Odd Harmonics of the Radiation from SASE FEL with Planar Undulator," *Proceedings of the 34th International Free Electron Laser Conference* (2012).
15. J. B. Murphy, C. Pellegrini, and R. Bonifacio, "Collective instability of a free electron laser including space charge and harmonics," Opt. Commun. **53**(3), 197–202 (1985).
16. E. Schneidmiller and M. Yurkov, *Background-free Harmonic Production in XFELs via a Reverse Undulator Taper* (JACOW, Geneva, Switzerland, 2017).
17. R. Y. Engel, P. S. Miedema, D. Turenne, *et al.*, "Parallel Broadband Femtosecond Reflection Spectroscopy at a Soft X-Ray Free-Electron Laser," Appl. Sci. **10**(19), 6947 (2020).
18. R. Kato, M. Fujimoto, T. Igo, *et al.*, "Characteristic measurements of higher harmonics generated in the SASE-FEL process," Nucl. Instrum. Methods Phys. Res., Sect. A **507**(1-2), 409–412 (2003).
19. A. Tremaine, X. J. Wang, M. Babzien, *et al.*, "Measurements of nonlinear harmonic radiation and harmonic microbunching in a visible SASE FEL," Nucl. Instrum. Methods Phys. Res., Sect. A **507**(1-2), 445–449 (2003).
20. S. DÜsterer, P. Radcliffe, G. Geloni, *et al.*, "Spectroscopic characterization of vacuum ultraviolet free electron laser pulses," Opt. Lett. **31**(11), 1750–1752 (2006).
21. T. M. Baumann, R. Boll, A. De Fanis, *et al.*, "Harmonic radiation contribution and X-ray transmission at the Small Quantum Systems instrument of European XFEL," J. Synchrotron Radiat. **30**(4), 662–670 (2023).
22. A. Tremaine, X. J. Wang, M. Babzien, *et al.*, "Experimental Characterization of Nonlinear Harmonic Radiation from a Visible Self-Amplified Spontaneous Emission Free-Electron Laser at Saturation," Phys. Rev. Lett. **88**(20), 204801 (2002).
23. G. Penco, G. Perosa, E. Allaria, *et al.*, "Nonlinear harmonics of a seeded free-electron laser as a coherent and ultrafast probe to investigate matter at the water window and beyond," Phys. Rev. A **105**(5), 053524 (2022).
24. C. Spezzani, A. Ravindran, E. Allaria, *et al.*, "Circular dichroism experiments at the *L* edge of magnetic transition metals enabled by elliptically polarized pulses from a seeded free-electron laser," Phys. Rev. B **110**(17), 174409 (2024).
25. R. Ivanov, M. M. Bidhendi, I. J. B. Macias, *et al.*, "Free-electron laser temporal diagnostic beamline FL21 at FLASH," Opt. Express **31**(12), 19146–19158 (2023).
26. M. Straub, T. Ding, M. Rebholz, *et al.*, "Differential Measurement of Electron Ejection after Two-Photon Two-Electron Excitation of Helium," Phys. Rev. Lett. **129**(18), 183204 (2022).
27. S. M. Durkan, V. Richardson, L. Varvarezos, *et al.*, "Multiphoton single and double ionization of neon in the EUV," J. Phys. B: At., Mol. Opt. Phys. **58**(1), 015601 (2025).
28. V. Richardson, J. T. Costello, D. Cubaynes, *et al.*, "Two-Photon Inner-Shell Ionization in the Extreme Ultraviolet," Phys. Rev. Lett. **105**(1), 013001 (2010).
29. D. Kutnyakhov, R. P. Xian, M. Dendzik, *et al.*, "Time- and momentum-resolved photoemission studies using time-of-flight momentum microscopy at a free-electron laser," Rev. Sci. Instrum. **91**(1), 013109 (2020).
30. A. P. Mancuso, T. Gorniak, F. Staier, *et al.*, "Coherent imaging of biological samples with femtosecond pulses at the free-electron laser FLASH," New J. Phys. **12**(3), 035003 (2010).
31. T. Gorniak, R. Heine, A. P. Mancuso, *et al.*, "X-ray holographic microscopy with zone plates applied to biological samples in the water window using 3rd harmonic radiation from the free-electron laser FLASH," Opt. Express **19**(12), 11059–11070 (2011).
32. C. Gutt, L.-M. Stadler, S. Streit-Nierobisch, *et al.*, "Resonant magnetic scattering with soft x-ray pulses from a free-electron laser operating at 1.59 nm," Phys. Rev. B **79**(21), 212406 (2009).
33. S. Hellmann, C. Sohrt, M. Beye, *et al.*, "Time-resolved x-ray photoelectron spectroscopy at FLASH," New J. Phys. **14**(1), 013062 (2012).
34. Z. Huang and K.-J. Kim, "Review of x-ray free-electron laser theory," Phys. Rev. Spec. Top.–Accel. Beams **10**(3), 034801 (2007).
35. D. Ratner, A. Brachmann, F. J. Decker, *et al.*, "Second and third harmonic measurements at the linac coherent light source," Phys. Rev. Spec. Top.–Accel. Beams **14**(6), 060701 (2011).
36. Z. Huang and K.-J. Kim, "Nonlinear harmonic generation of coherent amplification and self-amplified spontaneous emission," Nucl. Instrum. Methods Phys. Res., Sect. A **475**(1-3), 112–117 (2001).
37. E. L. Saldin, E. A. Schneidmiller, and M. V. Yurkov, "FAST: a three-dimensional time-dependent FEL simulation code," Nucl. Instrum. Methods Phys. Res., Sect. A **429**(1-3), 233–237 (1999).
38. M. M. Bidhendi, I. J. Bermudez Macias, R. Ivanov, *et al.*, "FEL Pulse Duration Evolution along Undulators at FLASH," Appl. Sci. **12**(14), 7048 (2022).
39. J. W. Goodman, *Statistical Optics*, 2nd Edition (Wiley, 2015).
40. E. L. Saldin, E. A. Schneidmiller, and M. V. Yurkov, "Statistical properties of radiation from VUV and X-ray free electron laser," Opt. Commun. **148**(4-6), 383–403 (1998).
41. E. L. Saldin, E. A. Schneidmiller, and M. V. Yurkov, *The Physics of Free Electron Lasers* (Springer, 2000).
42. E. L. Saldin, E. A. Schneidmiller, and M. V. Yurkov, "Scheme for attophysics experiments at a X-ray SASE FEL," Opt. Commun. **212**(4-6), 377–390 (2002).

Optics EXPRESS

43. E. L. Saldin, E. A. Schneidmiller, and M. V. Yurkov, "Coherence properties of the radiation from X-ray free electron laser," Opt. Commun. **281**(5), 1179–1188 (2008).
44. R. Bonifacio, C. Pellegrini, and L. M. Narducci, "Collective instabilities and high-gain regime in a free electron laser," Opt. Commun. **50**(6), 373–378 (1984).
45. R. Bonifacio, L. De Salvo, P. Pierini, *et al.*, "Spectrum, temporal structure, and fluctuations in a high-gain free-electron laser starting from noise," Phys. Rev. Lett. **73**(1), 70–73 (1994).
46. E. A. Schneidmiller and M. V. Yurkov, "Coherence Properties of the Radiation from X-ray Free Electron Lasers," CERN YR School Proc. **1**, 539 (2018).
47. H. P. Freund, S. G. Biedron, and S. V. Milton, "Nonlinear harmonic generation in free-electron lasers," IEEE J. Quantum Electron. **36**(3), 275–281 (2000).
48. C. Gerth, G. Brenner, M. Caselle, *et al.*, "Linear array detector for online diagnostics of spectral distributions at MHz repetition rates," J. Synchrotron Radiat. **26**(5), 1514–1522 (2019).
49. C. von Korff Schmising, F. Willems, S. Sharma, *et al.*, "Element-Specific Magnetization Dynamics of Complex Magnetic Systems Probed by Ultrafast Magneto-Optical Spectroscopy," Appl. Sci. **10**(21), 7580 (2020).
50. D. Mayer, F. Lever, D. Picconi, *et al.*, "Following excited-state chemical shifts in molecular ultrafast x-ray photoelectron spectroscopy," Nat. Commun. **13**(1), 198 (2022).
51. M. M. Bidhendi, G. Goetzke, I. J. Bermudez Macias, *et al.*, "Determination of the XUV Frequency Chirp at the Free-Electron Laser FLASH via THz Streaking and Electron Beam Diagnostics," Photonics **11**(12), 1153 (2024).
52. I. Zagorodnov and M. Dohlus, "Semianalytical modeling of multistage bunch compression with collective effects," Phys. Rev. Spec. Top.–Accel. Beams **14**(1), 014403 (2011).
53. U. FrÜhling, M. Wieland, M. Gensch, *et al.*, "Single-shot terahertz-field-driven X-ray streak camera," Nat. Photonics **3**(9), 523–528 (2009).
54. I. Grguraš, A. R. Maier, C. Behrens, *et al.*, "Ultrafast X-ray pulse characterization at free-electron lasers," Nat. Photonics **6**(12), 852–857 (2012).
55. U. Frühling, "Light-field streaking for FELs," J. Phys. B: At. Mol. Opt. Phys. **44**(24), 243001 (2011).
56. R. Ivanov, I. J. B. Macias, J. Liu, *et al.*, "Single-shot temporal characterization of XUV pulses with duration from ~10 fs to ~350 fs at FLASH," J. Phys. B: At. Mol. Opt. Phys. **53**(18), 184004 (2020).
57. K. Tiedtke, J. Feldhaus, U. Hahn, *et al.*, "Gas detectors for x-ray lasers," J. Appl. Phys. **103**(9), 094511 (2008).
58. M. Braune, J. Buck, M. Kuhlmann, *et al.*, "Non-invasive online wavelength measurements at FLASH2 and present benchmark," J. Synchrotron Radiat. **25**(1), 3–15 (2018).
59. R. Ivanov, J. Liu, G. Brenner, *et al.*, "FLASH free-electron laser single-shot temporal diagnostic: terahertz-field-driven streaking," J. Synchrotron Radiat. **25**(1), 26–31 (2018).
60. A. Azima, J. Bödewadt, O. Becker, *et al.*, "Direct measurement of the pulse duration and frequency chirp of seeded XUV free electron laser pulses," New J. Phys. **20**(1), 013010 (2018).
61. I. J. B. Macias, S. Düsterer, R. Ivanov, *et al.*, "Study of temporal, spectral, arrival time and energy fluctuations of SASE FEL pulses," Opt. Express **29**(7), 10491–10508 (2021).
62. U. Becker and D. A. Shirley, *VUV and Soft X-Ray Photoionization*, Physics of Atoms and Molecules (Springer, 1996), 1st ed.
63. M. Mehrjoo, B. Faatz, G. Paraskaki, *et al.*, *Expected Radiation Properties of the Harmonic Afterburner at FLASH2* (JACOW Publishing, 2019).
64. A. A. Sorokin, Y. Bican, S. Bonfigt, *et al.*, "An X-ray gas monitor for free-electron lasers," J. Synchrotron Radiat. **26**(4), 1092–1100 (2019).
65. P. Finetti, H. Höppner, E. Allaria, *et al.*, "Pulse Duration of Seeded Free-Electron Lasers," Phys. Rev. X **7**(2), 021043 (2017).
66. J. C. Diels and W. Rudolph, *Ultrashort Laser Pulse Phenomena* (Elsevier, Academic Press, 2006).